[Supplementary Materials]

Disease-specific primed human adult stem cells effectively ameliorate experimental atopic dermatitis in mice

Byung-Chul Lee[1], Jae-Jun Kim[1], Jin Young Lee[1], Insung Kang[1,§], Nari Shin[1], Seung-Eun Lee[1], Soon Won Choi[1], Je-Yoel Cho[2], Hyung-Sik Kim[3,4†], Kyung-Sun Kang[1†]

[1]Adult Stem Cell Research Center and Research Institute for Veterinary Science, College of Veterinary Medicine, Seoul National University, Seoul 08826, Republic of Korea

[2]Department of Biochemistry, BK21 PLUS Program for Creative Veterinary Science Research and Research Institute for Veterinary Science, College of Veterinary Medicine, Seoul National University, Seoul 08826, Republic of Korea

[3]Department of Life Science in Dentistry, School of Dentistry, Pusan National University, Yangsan 50612, Republic of Korea

[4]Institute for Translational Dental Sciences, Pusan National University, Yangsan 50612, Republic of Korea

[§]Current address: Program in Developmental Endocrinology and Genetics, Eunice Kennedy Shriver National Institute of Child Health and Human Development, NIH, Bethesda, MD 20892, USA

[†]Authors share co-corresponding authorship

Kyung-Sun Kang, D.V.M., Ph.D.

Adult Stem Cell Research Center, College of Veterinary Medicine, Seoul National University, 1 Gwanak-ro, Gwanak-gu, Seoul 08826, South Korea

Tel. +82-2-880-1246

E-mail: kangpub@snu.ac.kr

Hyung-Sik Kim, D.V.M., Ph.D.

Department of Life Science in Dentistry, School of Dentistry, Pusan National University, Yangsan 50612, Republic of Korea

Tel: +82-51-510-8231

E-mail: hskimcell@pusan.ac.kr

Supplementary Methods

Th2 cell isolation and polarization

Naïve $CD4^+$ T lymphocytes were isolated from PBMCs using a naïve $CD4^+$ T cell isolation kit (Miltenyi Biotec, Bergisch Gladbach, Germany) according to the manufacturer's instruction. Isolated cells were treated with 50 ng/ml of interleukin (IL)-2 and anti-CD3/28 beads for proliferation. For Th2 cell-specific polarization, 50 μg/ml of anti-IFN-γ, 25 ng/ml of IL-4 and 25 ng/ml of IL-6 were supplemented in the medium and cultured for 5 days in the presence of MC-primed hUCB-MSCs. Polarized Th2 cells were analyzed by detecting surface or intracellular markers using flow cytometry. For surface marker staining, Th2 cells were fixed and incubated with FITC-conjugated anti-CD4. For intracellular marker staining, cells were fixed and permeabilized with an intracellular staining buffer set (BD Biosciences, San Jose, CA, USA) and then incubated with PE-conjugated anti-IL-4 antibody. Detection was performed with a FACScalibur flow cytometer and evaluated using Cell Quest software (BD Bioscience).

Supplementary Figures

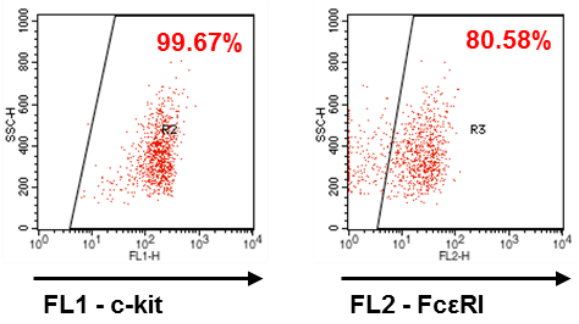

Figure S1. Cell surface marker expression of LAD2 cells. The expression of mast cell-specific markers, c-kit and FcεRI in LAD2 cells was measured by flow cytometric analysis. Results show a representative experiment.

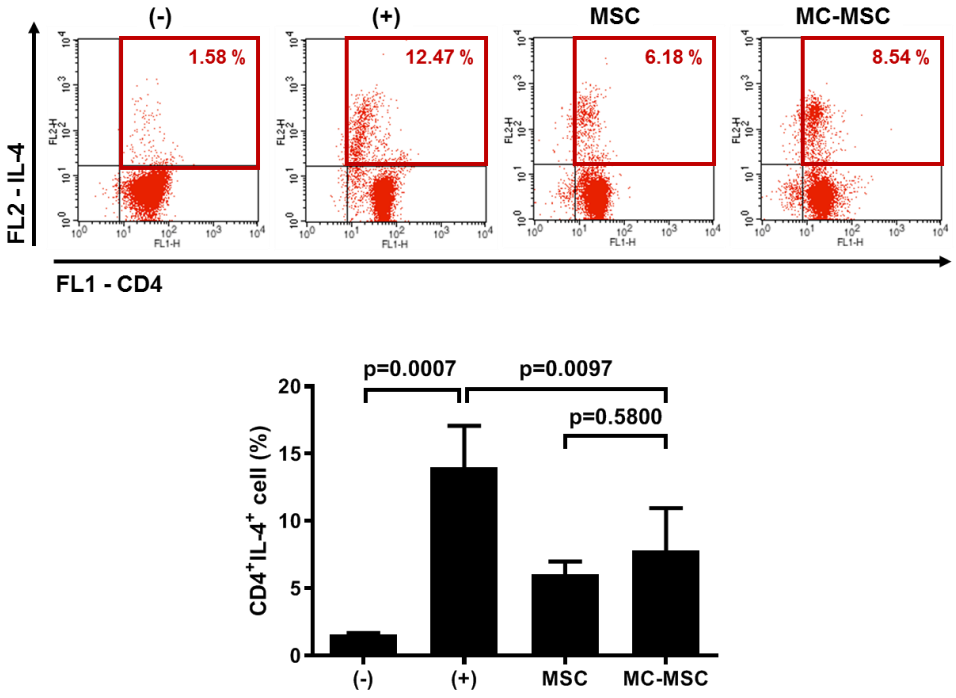

Figure S2. MC-primed hUCB-MSCs does not exert any significant change on the suppression of Th2 cells. Naïve $CD4^+$ T cells were isolated from PBMCs and cultured with anti-CD3/28 beads, 50 μg/ml anti-IFN-γ, 50 ng/ml IL-2, 25 ng/ml IL-4 and 25 ng/ml IL-6 for 5 days. The expression of cellular markers were determined by flow cytometric analysis. (-): Negative control group, (+): Th2 polarized cell group, MSC: hUCB-MSC co-cultured group, MC-MSC: MC-primed hUCB-MSC co-cultured group. *In vitro* experiments were performed in triplicate, using hUCB-MSCs isolated from each different donor (N=3). The results are shown as the mean ± SD.

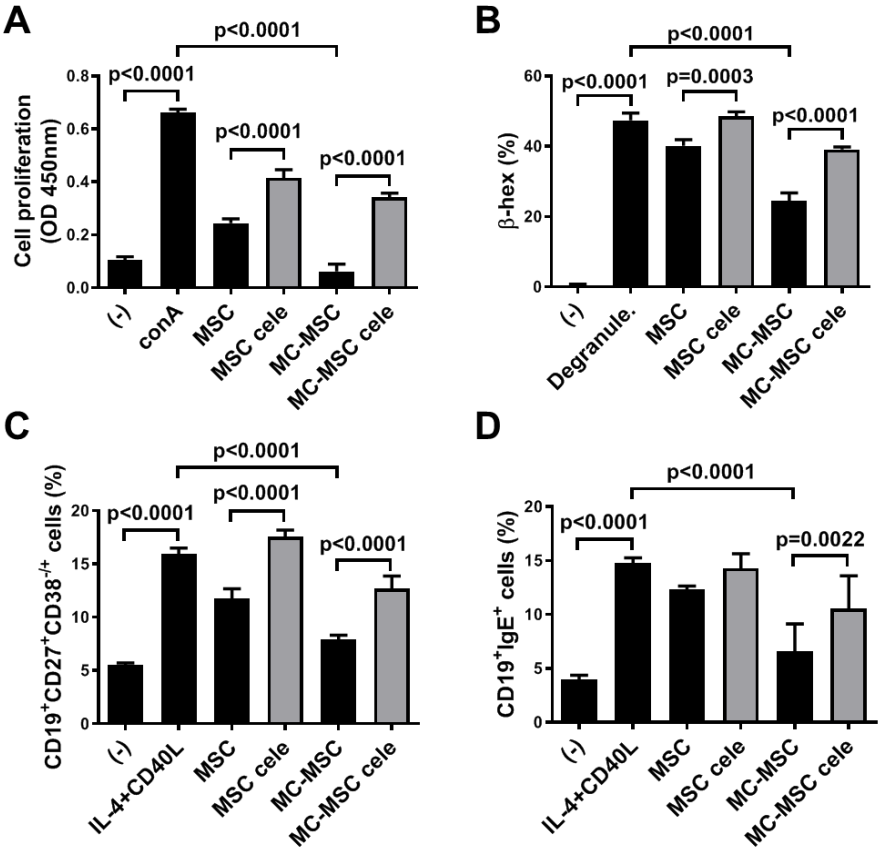

Figure S3. Selective inhibition of COX-2 impedes the suppressive effect of MC-primed hUCB-MSCs on activation of disease-related immune cells. (A) Immunosuppressive properties of primed hUCB-MSCs were determined by the MLR assay. **(B)** After co-culture with hUCB-MSCs during the sensitization period (24 h), LAD-2 cells were challenged with anti-IgE (3 μg/ml). The degranulation rate of LAD2 cells was assessed by detecting β-hexosaminidase in the cultured medium. **(C-D)** Naïve B lymphocytes were isolated from hPBMCs and cultured for 5 days in medium supplemented with CD40L (100 ng/ml) and IL-4 (25 ng/ml) in the presence of MC-primed hUCB-MSCs. Maturation **(C)** and IgE production **(D)** were determined by flow cytometric analysis. *In vitro* experiments were performed in triplicate, using hUCB-MSCs isolated from each different donor (N=3). The results are shown as the mean ± SD.

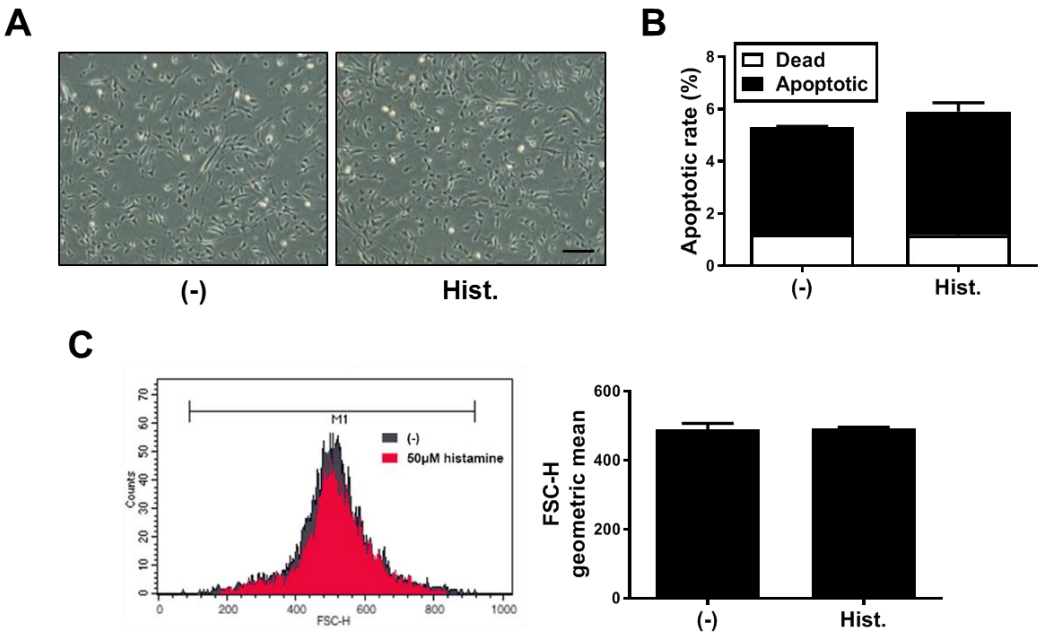

Figure S4. Histamine treatment does not induce toxic effect on hUCB-MSCs. hUCB-MSCs were treated with 50 μM histamine for 24 h. **(A)** Morphological change after the histamine treatment was observed by microscope, bar = 100 μm. **(B-C)** Apoptosis **(B)** and cell size **(C)** were determined by flow cytometric analysis. *In vitro* experiments were performed in triplicate, using hUCB-MSCs isolated from each different donor (N=3). The results are shown as the mean ± SD.

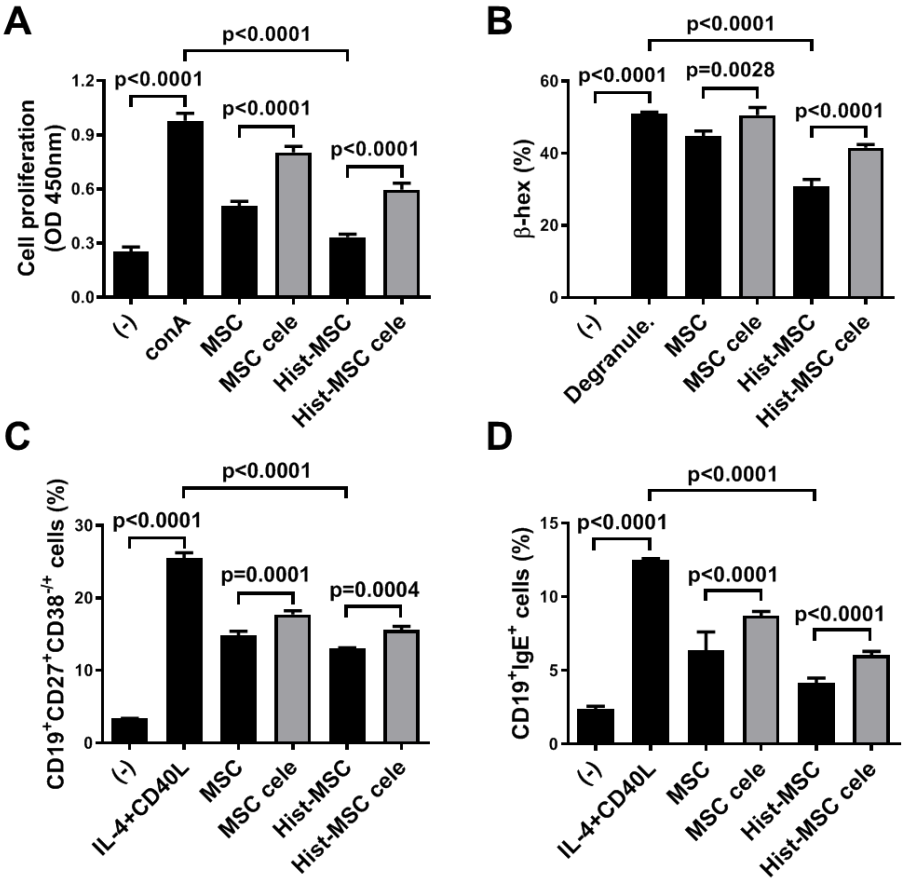

Figure S5. Selective inhibition of COX-2 hinders the immunomodulatory function of histamine-treated hUCB-MSCs. (A) Immunosuppressive properties of primed hUCB-MSCs were determined by the MLR assay. **(B)** After co-culture with hUCB-MSCs during the sensitization period (24 h), LAD-2 cells were challenged with anti-IgE (3 μg/ml). The degranulation rate of LAD2 cells was assessed by detecting β-hexosaminidase in the cultured medium. **(C-D)** Naïve B lymphocytes were isolated from hPBMCs and cultured for 5 days in medium supplemented with CD40L (100 ng/ml) and IL-4 (25 ng/ml) in the presence of histamine-treated hUCB-MSCs. Maturation **(C)** and IgE production **(D)** were determined by flow cytometric analysis. *In vitro* experiments were performed in triplicate, using hUCB-MSCs isolated from each different donor (N=3). The results are shown as the mean ± SD.

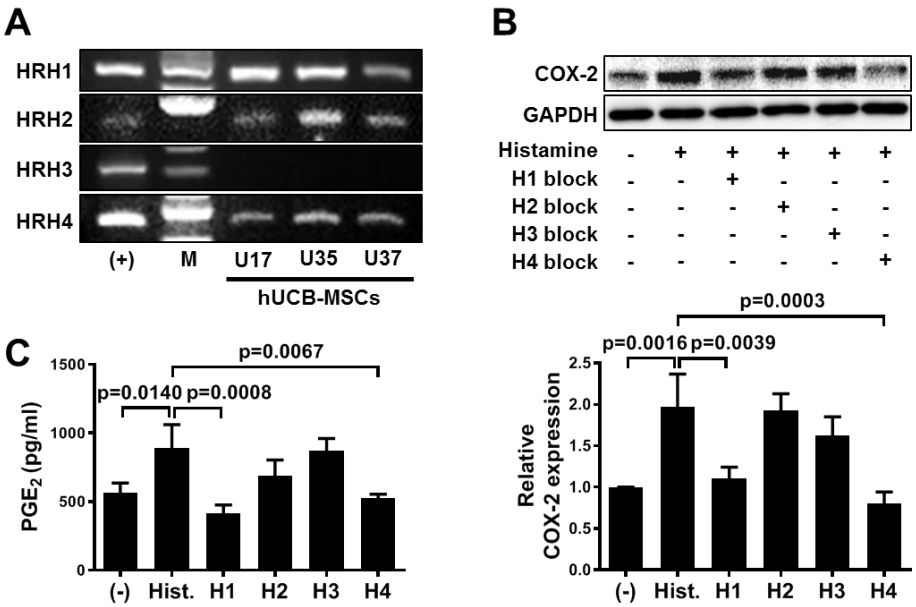

Figure S6. The expression pattern of histamine receptors in hUCB-MSCs and its role in COX-2~PGE_2 axis. (A) The expression of histamine receptor subtypes were determined by PCR and gel electrophoresis. Positive control for H1, 2 and 4: HT29 cell, H3: HeLa cell. **(B-C)** In the presence of histamine, inhibitory effect of subtype-specific antagonists for histamine receptors on the expression of COX-2 **(B)** and secretion of PGE_2 **(C)** were assessed by western blot analysis and ELISA, respectively. Blockers for H1: diphenhydramine hydrochloride, H2: cimetidine, H3: ciproxifan hydrochloride, H4: JNJ7777120. *In vitro* experiments were performed in triplicate, using hUCB-MSCs isolated from each different donor (N=3). The results are shown as the mean ± SD.

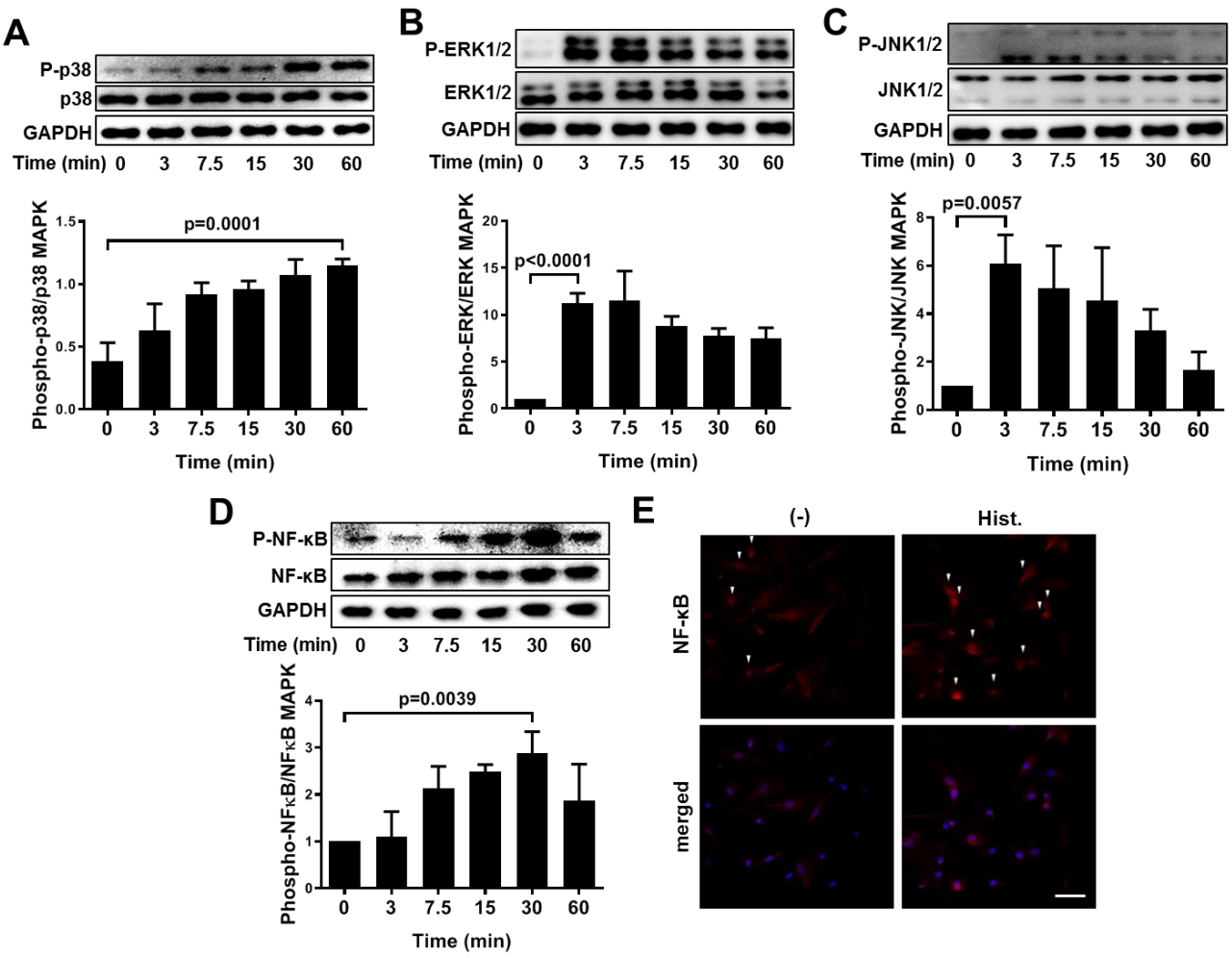

Figure S7. Histamine activates NF-κB pathway of hUCB-MSCs to upregulate COX-2 signaling. (A-D) hUCB-MSCs were treated with 50 μM histamine and cell lysates were collected at each indicated time point. Time-dependent phosphorylation of P(Thr^{180}/Tyr^{182})-p38 **(A)**, P(Thr^{202}/Tyr^{204})-ERK1/2 **(B)**, P(Thr^{183}/Tyr^{185})-JNK1/2 **(C)** and P(SER^{536})-NF-κB **(D)** in histamine-treated hUCB-MSCs was determined by western blot analysis and quantified. **(E)** Immunocytochemistry analysis of NF-κB after treatment with histamine, bar = 100 μm. *In vitro* experiments were performed in triplicate, using hUCB-MSCs isolated from each different donor (N=3). The results are shown as the mean ± SD.

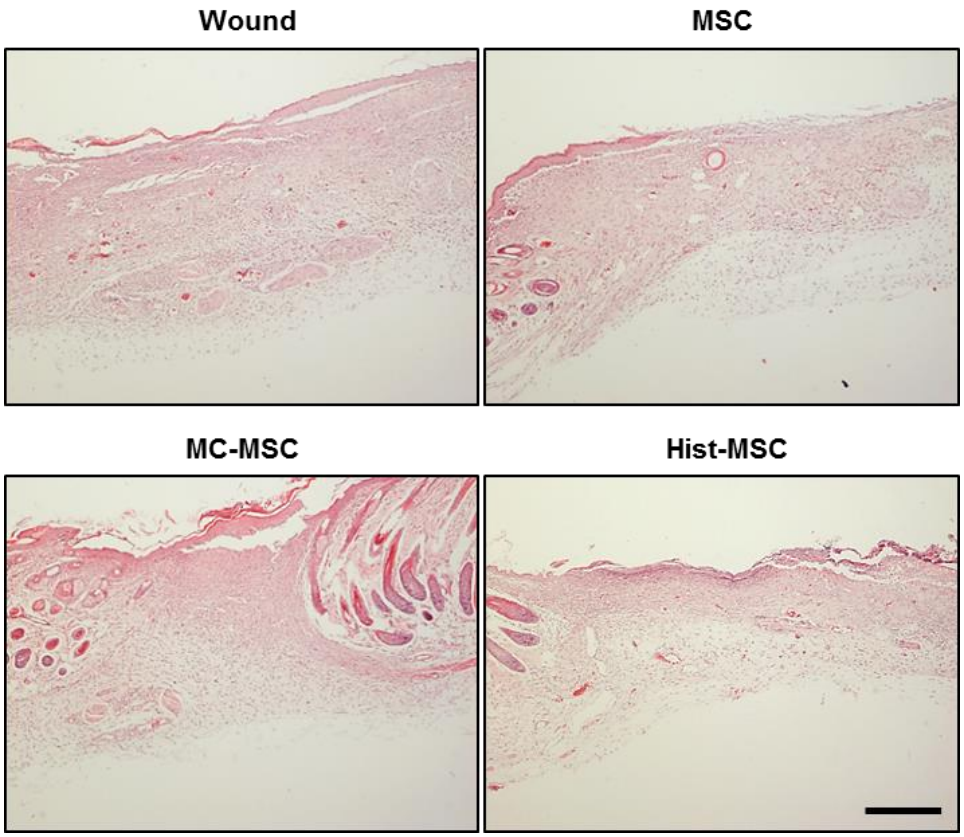

Figure S8. MC granule-primed hUCB-MSCs ameliorate histopathological symptoms in dorsal skin of excisional wound mice more efficiently than naïve and histamine-treated cells. The dorsal skin of BALB/c mice was punched with a 5-mm-diameter biopsy punch, and 1×10^6 MC-primed hUCB-MSCs were immediately infused subcutaneously. Each group of mice was monitored and sacrificed on day 14 for further *ex vivo* examinations. Representative H&E-stained images of dorsal skin (n=5), bar = 500 μm. Wound: Excisional wound mice group, MSC: hUCB-MSC-injected group, MC-MSC: MC-primed hUCB-MSC-injected group, Hist-MSC: histamine-treated hUCB-MSC-injected group.